Journal of Power Sources 196 (2011) 3325–3330

Contents lists available at ScienceDirect

Journal of Power Sources

journal homepage: www.elsevier.com/locate/jpowsour

Ag_xVOPO_4: A demonstration of the dependence of battery-related electrochemical properties of silver vanadium phosphorous oxides on Ag/V ratios

Young Jin Kim [a], Chia-Ying Lee [a], Amy C. Marschilok [a,b,c], Kenneth J. Takeuchi [c], Esther S. Takeuchi [a,b,c,d,*]

[a] Department of Chemical and Biological Engineering, University at Buffalo (SUNY), Buffalo, NY 14260, United States
[b] Department of Electrical Engineering, University at Buffalo (SUNY), Buffalo, NY 14260, United States
[c] Department of Chemistry, University at Buffalo (SUNY), Buffalo, NY 14260, United States
[d] Department of Biomedical Engineering, University at Buffalo (SUNY), Buffalo, NY 14260, United States

ARTICLE INFO

Article history:
Received 1 November 2010
Received in revised form
24 November 2010
Accepted 26 November 2010
Available online 2 December 2010

Keywords:
Silver vanadium phosphorous oxide
Cathode
Lithium battery
Primary battery
Implantable medical device
Electrochemical reduction

ABSTRACT

As a part of our on-going study on silver vanadium phosphorous oxides ($Ag_xV_yO_zPO_4$), we report here the first study of the electrochemical reduction of a low Ag/V ratio silver vanadium phosphorous oxide, $Ag_{0.48}VOPO_4{\cdot}1.9H_2O$. Reminiscent of $Ag_2VO_2PO_4$ reduction, *in situ* formation of silver metal nanoparticles along with an associated increase in conductivity were observed after reduction of $Ag_{0.48}VOPO_4{\cdot}1.9H_2O$ with 0.37 electron equivalents. However, in contrast to our lithium/$Ag_2VO_2PO_4$ cells, our lithium/$Ag_{0.48}VOPO_4{\cdot}1.9H_2O$ cells displayed an even higher voltage on discharge and a characteristic multi-plateau voltage profile, where vanadium reduction was the first reduction step.

1. Introduction

An on-going theme in our battery related research is the rational study of a new family of materials, namely silver vanadium phosphorous oxides ($Ag_xV_yO_zPO_4$), which have a chemical composition inspired by two commercially successful battery materials, $LiFePO_4$ and $Ag_2V_4O_{11}$. Phosphate based materials have been successfully implemented as cathodes for lithium batteries with the most notable phosphate cathode material being lithium iron phosphate ($LiFePO_4$) [1,2]. Phosphate materials display impressive electrochemical stability, but a notable liability associated with phosphate materials is low conductivity. Silver vanadium oxide ($Ag_2V_4O_{11}$) has been a cathode material of choice for batteries that power implantable cardiac defibrillators over the past 20 years [3,4]. Reminiscent of other vanadium oxides, $Ag_2V_4O_{11}$ exhibits high voltage in lithium based batteries [5]. Further, the bimetallic (Ag, V) composition allows multiple electron reduction per $Ag_2V_4O_{11}$ formula unit, resulting in high capacity. The discharge of silver vanadium oxide progresses with a significant increase in cathode conductivity consistent with *in situ* formation of silver metal nanoparticles upon reduction of Ag^+ to Ag^0 [6]. Further, silver vanadium oxide displays a complex voltage profile upon electrochemical reduction, with several distinct plateaus useful for end-of-service indication in lithium based silver vanadium oxide implantable cardiac defibrillator batteries.

The desire to address the low conductivity observed in phosphate based cathode materials with an *in situ* generation of a conductive matrix, while providing high operating voltage, high capacity, and clear end-of-service indication led to our deliberate selection of silver vanadium phosphorous oxides (SVPO) for exploration as new cathode materials for lithium based batteries. We recently introduced the first member of the silver vanadium phosphorous oxide family for electrochemical study, $Ag_2VO_2PO_4$. When used as a cathode in a lithium based battery, $Ag_2VO_2PO_4$ displayed high discharge capacity and high current pulse capability, both promising attributes toward future use in high power biomedical applications [7]. The chemical changes in the $Ag_2VO_2PO_4$ cathode as a function of discharge were examined [8]. Most notably, as reduction was initiated, *in situ* formation of silver nanoparticles in the cathode matrix was observed with an accompanying 15,000 fold increase in cathode conductivity. The impact of discharge on the resistance and impedance behavior of the cell was also studied [9]. We also reported a novel ambient pressure synthesis method for $Ag_2VO_2PO_4$ preparation with accompanying changes in morphology, particle size, and surface area over the previously

* Corresponding author at: 303 Furnas Hall, University at Buffalo, Buffalo, NY 14260, United states. Tel.: +1 716 645 1185; fax: +1 716 645 3822.
E-mail address: et23@buffalo.edu (E.S. Takeuchi).

0378-7753/$ – see front matter © 2010 Elsevier B.V. All rights reserved.
doi:10.1016/j.jpowsour.2010.11.144

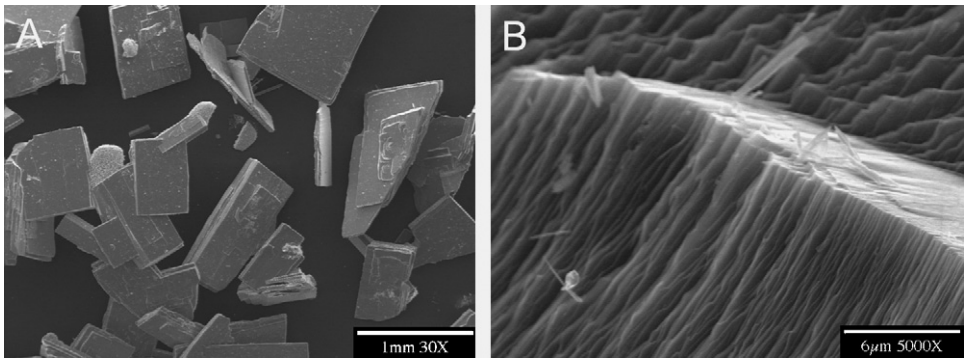

Fig. 1. Scanning electron micrograph of as prepared $Ag_{0.48}VOPO_4{\cdot}1.9H_2O$ under (A) 30× and (B) 5000× magnification.

reported preparation method providing enhanced behavior under pulse discharge conditions [10]. While $Ag_2VO_2PO_4$ exhibited several desirable characteristics, two possible opportunity areas were still apparent: higher operating voltage and a voltage profile providing the possibility for direct state of discharge determination.

We report here the first electrochemical study of an alternate composition SVPO material, $Ag_{0.48}VOPO_4$. Notably, this material has a lower silver content, with a silver to vanadium ratio, Ag/V, of <0.5 compared to a Ag/V ratio of 2.0 for the previously studied material, $Ag_2VO_2PO_4$. Lithium/$Ag_{0.48}VOPO_4{\cdot}1.9H_2O$ electrochemical cells show a high operating voltage and a characteristic multi-plateau voltage profile, both potentially desirable properties for use in implantable medical devices. Stepwise characterisation of the discharged $Ag_{0.48}VOPO_4{\cdot}1.9H_2O$ material by X-ray diffraction, scanning electron microscopy, and four-point conductivity measurements is conducted to probe the discharge mechanism. The reduction mechanism for $Ag_{0.48}VOPO_4$ is contrasted with that of $Ag_2VO_2PO_4$ and rationalized on the basis of structural and chemical differences in the two SVPO materials. This work contributes to the ability to tune electrochemical properties of cathode materials, including bimetallic phosphates, by control of chemical composition and structure.

2. Experimental

$Ag_{0.48}VOPO_4{\cdot}1.9H_2O$ was prepared following a previously reported hydrothermal synthesis method [11]. Scanning electron microscope (SEM) images were taken using a Hitachi SU-70 field emitting scanning electron microscope. Powder X-ray diffraction (XRD) was performed using a Rigaku Ultima IV X-ray diffractometer equipped with CuKα radiation, Bragg–Brentano geometry, and a monochromator. A high temperature stage enabling *in situ* XRD measurements at elevated temperature was also utilized. As-collected XRD patterns were analysed using MDI JADE 8 software. Inductively coupled plasma atomic emission spectroscopy (ICP-AES) was performed using a Thermo Scientific iCAP 6000 series ICP spectrometer. Thermogravimetric analysis (TGA) was performed using a TA Instruments SDT Q600, and water content was calculated based on total weight lost between room temperature and 500 °C. True density was measured using a Micromeritics AccuPyc II 1340 pycnometer using He gas. Four point conductivity measurements were taken using a standard linear four-point probe arrangement.

Lithium anodes were used in coin type experimental cells with 1 M $LiAsF_6$ in propylene carbonate and dimethoxyethane (1:1 by volume) as the electrolyte. $Ag_{0.48}VOPO_4{\cdot}1.9H_2O$ material was used as synthesized or combined with conductive carbon to form cathodes. Discharge tests were performed at 37 °C at a current density of 0.07–0.08 mA cm^{-2}. Some cathodes were recovered for further *ex situ* XRD, SEM, and four-point conductivity characterisation after the cells reached the desired level of discharge.

3. Results

Scanning electron micrographs of the as prepared $Ag_{0.48}VOPO_4{\cdot}nH_2O$ were recorded (Fig. 1). The hydrothermal preparation yielded millimeter sized bladed material (Fig. 1A). Examination of the particles under higher magnification revealed a layered morphology (Fig. 1B) where the particles appear to be comprised of rectangular stacked plates.

The stoichiometry of the prepared material was investigated in detail using a combination of inductively coupled plasma spectroscopy atomic emission spectroscopy (ICP) and thermogravimetric analysis (TGA). Determination of the silver to vanadium ratio by ICP showed a ratio of Ag/V of 0.48, slightly higher silver content than the Ag/V of 0.43 reported in the original preparation [11]. Assuming full incorporation of the silver into the V-O-P-O structure, the resulting formula of our material would be assigned as $Ag_{0.48}VOPO_4$. Due to the layered V-O-P-O structure and the use of water as a solvent during the hydrothermal synthesis process, some water is retained within the $Ag_{0.48}VOPO_4$ material. Therefore, weight loss as determined by thermogravimetric analysis was used to quantitatively assign the water content of our as-prepared material (Fig. 2). The average of several measurements showed a weight loss consistent with a water content of 1.9 water molecules per formula unit. Therefore, the final composition of our material was assigned to be $Ag_{0.48}VOPO_4{\cdot}1.9H_2O$.

Crystallographic information shows that $Ag_{0.43}VOPO_4{\cdot}2H_2O$ has a layered structure, with Ag^+ and H_2O between the layers (Fig. 3A) [11]. A similarity with the structure of $Ag_2VO_2PO_4$ (Fig. 3B) is the presence of V-O-P-O layers perpendicular to the *c*-axis with Ag^+ located between the layers. In both cases the silver is 6 coordinate in a distorted octahedral coordination environment [11,12]. However, in $Ag_2VO_2PO_4$ five of the oxygen atoms bonded to the

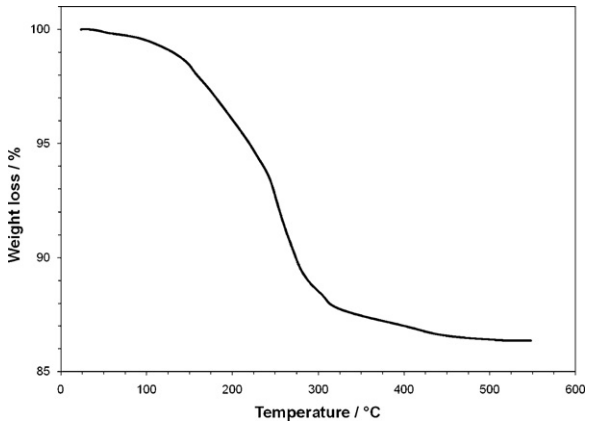

Fig. 2. Thermogravimetric analysis of as prepared $Ag_{0.48}VOPO_4{\cdot}1.9H_2O$.

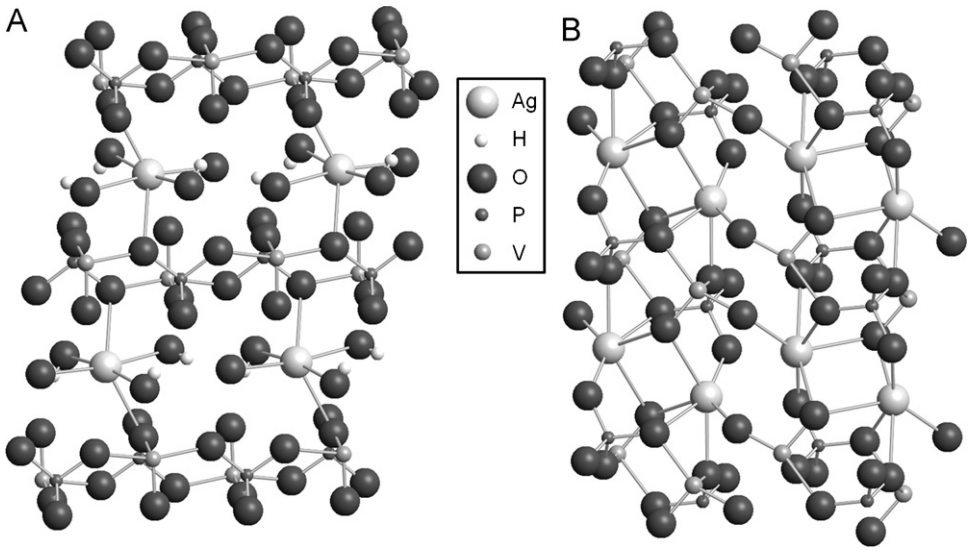

Fig. 3. Comparison of the coordination geometry of silver in (A) $Ag_{0.43}VOPO_4{\cdot}2H_2O$ and (B) $Ag_2VO_2PO_4$.

silver are shared with a vanadium center while in the case of $Ag_{0.43}VOPO_4{\cdot}2H_2O$ four of the oxygen atoms bonded to the silver are from the water molecules that are held between the vanadium phosphorous oxygen layers. The true density of our $Ag_{0.48}VOPO_4{\cdot}1.9H_2O$ material was measured to be 3.25 g cm^{-3}, ~40% less than that of $Ag_2VO_2PO_4$ (5.32 g cm^{-3}) [7].

To investigate structural changes as a function of temperature, *in situ* XRD measurements were recorded as the $Ag_{0.48}VOPO_4{\cdot}1.9H_2O$ material was heated and cooled. In the first set of *in situ* XRD measurements, $Ag_{0.48}VOPO_4{\cdot}1.9H_2O$ material was successively heated in 10 °C increments to 70 °C, then cooled back to room temperature (Fig. 4A). No significant crystallographic changes occurred as a result of heating. In a second set of *in situ* XRD measurements, the $Ag_{0.48}VOPO_4{\cdot}1.9H_2O$ material was successively heated from 80 °C to 100 °C, then cooled back to room temperature (Fig. 4B). In this case, new peaks emerged at temperatures ≥90 °C, and these peaks remained upon cooling back to room temperature. Since the material underwent irreversible crystallographic changes upon dehydration, the electrochemistry of the dehydrated $Ag_{0.48}VOPO_4$ could not be investigated.

The electrochemistry of $Ag_{0.48}VOPO_4{\cdot}1.9H_2O$ was examined by reduction of the material versus lithium metal in an experimental cell. Since the cathode material used for electrochemical experiments was consistently handled at temperatures <80 °C, no significant water loss occurred and the stoichiometry $Ag_{0.48}VOPO_4{\cdot}1.9H_2O$ was assigned for our electroactive cathode material. The cells were discharged under constant current, and complete voltage profiles are shown along with specific capacity and electron equivalents for the discharge (Fig. 5A). The discharge curve showed two voltage plateaus, the first at 3.7 V and second at 3.2 V. The first higher voltage plateau is consistent with reduction by ~0.3 electron equivalents per formula unit, while the second plateau is consistent with ~0.6 electron equivalents. Thus, the overall reduction of $Ag_{0.48}VOPO_4{\cdot}1.9H_2O$ takes place by the addition of ~0.9 electron equivalents in the two plateaus and a total of 1.26 electrons above 2.0 V. The characteristic voltage profile with the existence of multiple plateaus is often a useful characteristic for applications requiring state of discharge indication, such as implantable medical devices.

The voltage profile and specific energy of lithium cells containing $Ag_{0.48}VOPO_4{\cdot}1.9H_2O$ was compared with that of cells containing $Ag_2VO_2PO_4$ (Fig. 5B). Operating voltages of the $Ag_{0.48}VOPO_4{\cdot}1.9H_2O$ material were significantly higher, with >300 mWh g^{-1} delivered above 2.9 V. Notably, the $Ag_{0.48}VOPO_4$ material displayed initial voltages even higher those of $Ag_2V_4O_{11}$ [5]. In a comparison of one formula unit for each material, the average electronegativity per atom increases in the order $Ag_2VO_2PO_4 < Ag_2V_4O_{11} < Ag_{0.48}VOPO_4$, consistent with the observed trend in operating voltage.

In order to probe the reduction mechanism of $Ag_{0.48}VOPO_4{\cdot}1.9H_2O$ recovered cathodes were analysed at several states of discharge. Scanning electron micrographs of partially reduced silver vanadium phosphorous oxide (109 mAh g^{-1}, $x = 1.0$) were obtained (Fig. 6). Similar to the as-prepared material (Fig. 1),

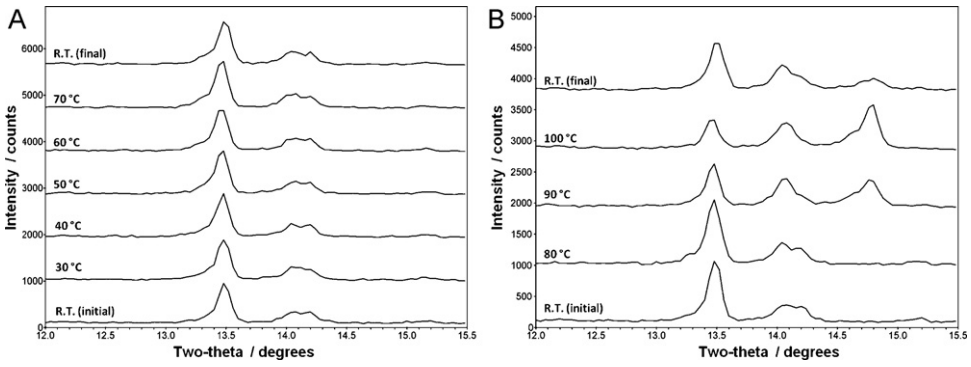

Fig. 4. *In situ* X-ray powder diffraction of heated $Ag_{0.48}VOPO_4{\cdot}1.9H_2O$ at temperatures ranging from (A) room temperature to 70 °C and (B) room temperature to 100 °C.

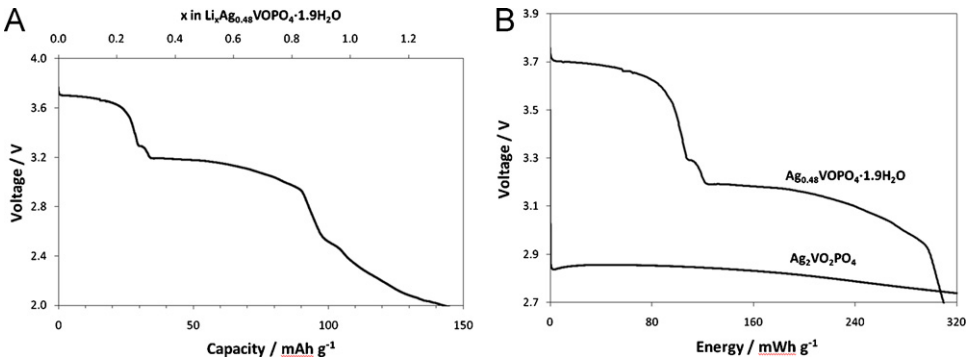

Fig. 5. Discharge of lithium/$Ag_{0.48}VOPO_4 \cdot 1.9H_2O$ experimental cells showing the (A) voltage curve under constant current discharge and (B) comparison with lithium/$Ag_2VO_2PO_4$ experimental cells under constant current discharge.

the layered nature of the particle can be seen in the SEM image of the discharged material (Fig. 6), showing that there is no gross degradation of the material upon electrochemical reduction. Superimposed on the layers are bright nanosized particles which were identified as silver by energy dispersive X-ray spectroscopy (EDS). The typical size of the parent silver particles ranged from 200 to 400 nm. It is also apparent from the location of the silver nanoparticles that the silver metal forms preferentially along the edges of the particles defined by the stacked plates. The SEM results do not indicate silver metal formation on the flat planar surfaces of the particles. This observation is consistent with ionic movement between the planes of the V–O–P–O layers.

Ex situ X-ray diffraction (XRD) measurements of the $Ag_{0.48}VOPO_4 \cdot 1.9H_2O$ cathodes were taken in order to interrogate phase changes in the material as a function of electrochemical reduction (Fig. 7). Several factors in the reduction process are notable. While the intensities in the XRD pattern of the original $Ag_{0.48}VOPO_4 \cdot 1.9H_2O$ material decrease, the formation of new phases can also be observed. In contrast to $Ag_2VO_2PO_4$ which becomes significantly more amorphous on discharge [8], the $Ag_{0.48}VOPO_4 \cdot 1.9H_2O$ material undergoes structural changes but exhibits a less significant loss in crystallinity. Further, while $Ag_2VO_2PO_4$ does not demonstrate significant constriction of the vanadium phosphorous oxygen layers on reduction [9], a significant constriction is observed with $Ag_{0.48}VOPO_4 \cdot 1.9H_2O$. In particular, the (0 0 2) peak at 13.5° 2-theta shifts to higher 2-theta values and a new peak appears after reduction by 0.37 electron equivalents (Fig. 8A). The shift in the 2-theta value indicates a decrease in the interlayer spacing of the vanadium phosphorous oxygen layers in the $Ag_{0.48}VOPO_4 \cdot 1.9H_2O$ structure. The most significant change in d-spacing was observed as the reduction progressed from the addition of 0.56–0.74 electron equivalents (Fig. 8B).

Li_xVOPO_4 undergoes significant distortion upon electrochemical reduction from V^{5+} to V^{4+}, so there is precedent for structural change in related materials as a function of state of lithiation [13]. However, in this case the significant constriction in the vanadium phosphorous oxygen interlayer spacing of $Ag_{0.48}VOPO_4 \cdot 1.9H_2O$ beyond 0.56 electron equivalents may also be related to the presence of water between the V–O–P–O layers. Notably, the silver ions located between the vanadium phosphorous oxygen layers are bonded at four of their six coordination sites to water (Fig. 3A) [11]. Thus, when the silver ions are reduced to silver metal the silver ion and the bound water may both exit the sites between the layers resulting in constriction of the vanadium phosphorous oxygen layers.

In order to further interrogate the electrochemical reduction mechanism, the decrease in the intensity of the (0 0 4) peak (highest intensity peak) of the parent $Ag_{0.48}VOPO_4 \cdot 1.9H_2O$ was plotted along with the increase in the intensity of the silver (1 1 1) peak as a function of state of reduction (Fig. 9). With the onset of reduction there is a rapid initial decrease in the (0 0 4) peak intensity of the parent material, where the (0 0 4) intensity continues to decrease up to 0.74 electron equivalents. However, only a minor amount of silver metal is detected on initial reduction with the majority of the silver metal formed after the addition of more than 0.5 electron

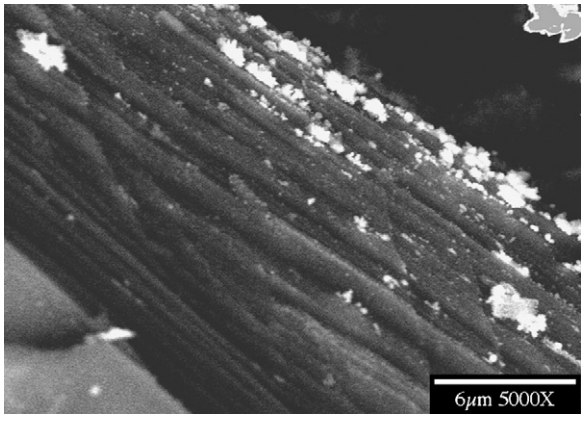

Fig. 6. Scanning electron micrograph of $Ag_{0.48}VOPO_4 \cdot 1.9H_2O$ electrochemically reduced by 1 electron equivalent.

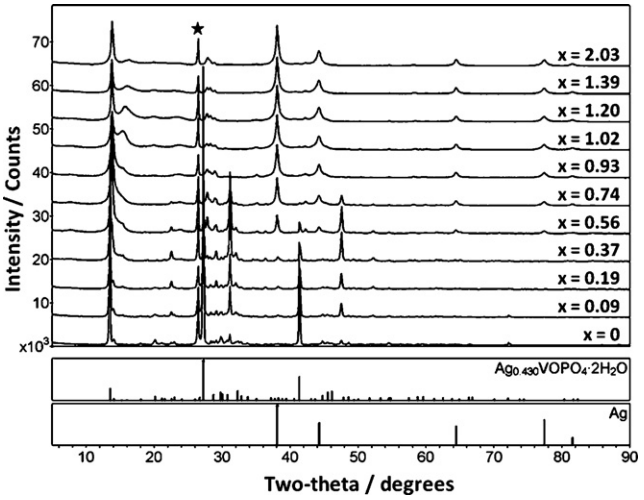

Fig. 7. XRD of reduced $Li_xAg_{0.48}VOPO_4 \cdot 1.9H_2O$ where *x* indicates the electron equivalents added. Reference patterns are shown for starting material and silver metal. Star indicates (0 0 2) peak for graphite.

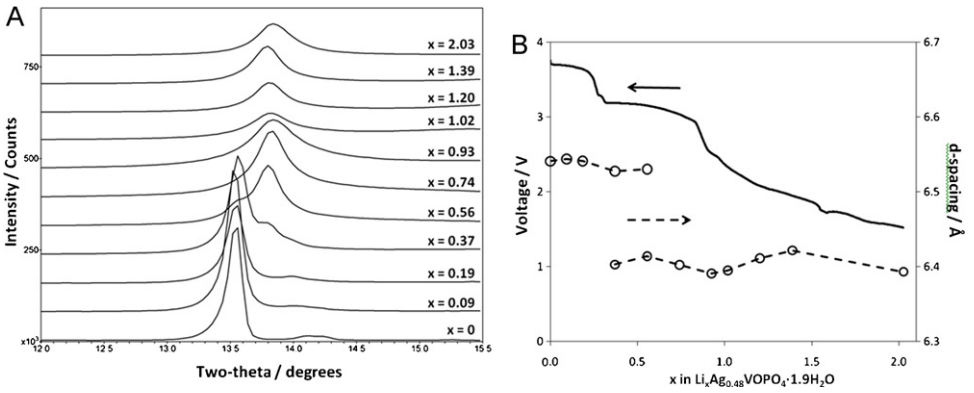

Fig. 8. *Ex situ* X-ray powder diffraction of electrochemically reduced $Ag_{0.48}VOPO_4 \cdot 1.9H_2O$. (A) 2-Theta position of the (0 0 2) peak for $Li_xAg_{0.48}VOPO_4 \cdot 1.9H_2O$ as a function of reduction. (B) Interlayer (d-spacing) of the (0 0 2) peak as a function of electron equivalents added. The voltage curve of lithium/$Ag_{0.48}VOPO_4 \cdot 1.9H_2O$ is shown for reference.

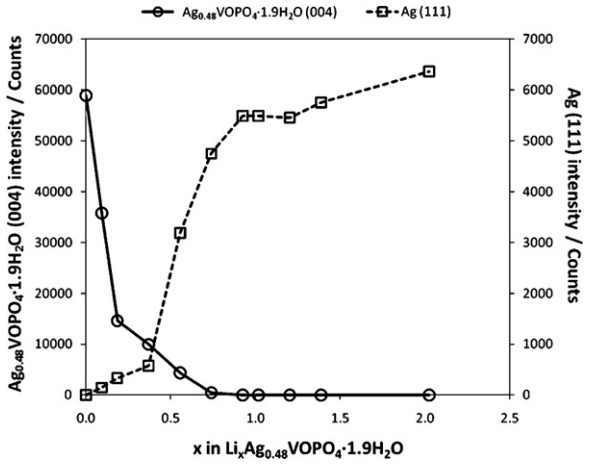

Fig. 9. Peak intensity of the (0 0 4) peak for $Li_xAg_{0.48}VOPO_4 \cdot 1.9H_2O$ and peak intensity of silver metal (1 1 1) as a function of reduction.

equivalents. This observed behavior is in contrast to the behavior of $Ag_2VO_2PO_4$ where the formation of silver metal is the initial predominant reduction process [8].

Four point probe data was collected to assess conductivity changes in the $Ag_{0.48}VOPO_4 \cdot 1.9H_2O$ pellet composite cathodes as a function of discharge (Fig. 10). Conductivity remained unchanged upon initial reduction to 0.37 electron equivalents, a significant > 20

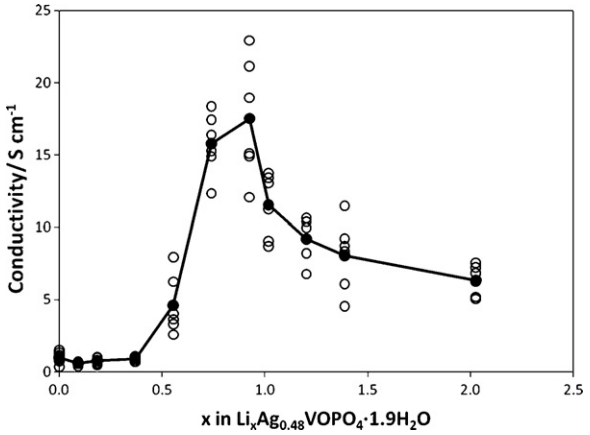

Fig. 10. Four point conductivity of $Li_xAg_{0.48}VOPO_4 \cdot 1.9H_2O$ composite cathodes pellets as a function of reduction, where open symbols are individual measurements and filled symbols are averages.

$$(1)\ Ag_{0.48}VOPO_4 \xrightarrow{xLi\ (x \le 0.52)} Li_xAg_{0.48}VOPO_4$$

$$(2)\ Li_xAg_{0.48}VOPO_4 \xrightarrow{yLi\ (y \le 0.48)} Li_{0.52+y}Ag_{0.48-y}VOPO_4 + yAg^0$$

$$(3)\ Li_{0.5+y}Ag_{0.48-y}VOPO_4 + yAg^0 \xrightarrow{zLi\ (z \le 0.26)} Li_{1.00+z}VOPO_4 + 0.48Ag^0$$

Scheme 1. Discharge mechanism of $Ag_{0.48}VOPO_4 \cdot 1.9H_2O$.

fold increase was observed upon further reduction to 0.93 electron equivalents. The conductivity data supports our XRD observation that initially reduction of V^{5+} to V^{4+} is preferred over reduction of Ag^+ to Ag^0.

The electrochemical reduction of $Ag_{0.48}VOPO_4 \cdot 1.9H_2O$ requires a total of 1.26 electron equivalents above 2.0 V (Fig. 5A). Based upon the SEM, XRD, and conductivity data discussed above, a three step mechanism is described. The reduction by ~1.00 electron equivalents is consistent with (1) the reduction of 0.52 equivalents of V^{5+} to V^{4+} followed by (2) the reduction of 0.48 equivalents of Ag^+ to Ag^0. The presence of one V^{4+} site is assigned for each Ag^+ ion to maintain electroneutrality. Further reduction to 1.26 electron equivalents would be consistent with an additional reduction of (3) 0.26 equivalents of V^{4+} to V^{3+}. This discharge mechanism is summarized (Scheme 1). It is important to note that the stoichiometry of the material prior to discharge was assigned as $Ag_{0.48}VOPO_4 \cdot 1.9H_2O$. It is possible that water is liberated during the discharge process which would be consistent with the smaller d-spacing observed for the discharged material.

4. Summary

This paper reports the first study of electrochemical reduction of silver vanadium phosphorous oxide $Ag_{0.48}VOPO_4 \cdot 1.9H_2O$. Lithium/$Ag_{0.48}VOPO_4 \cdot 1.9H_2O$ electrochemical cells showed a high operating voltage and a characteristic multi-plateau voltage profile, both potentially desirable properties for use as power sources in implantable medical devices. Analysis of discharged cathodes indicated that the significant formation of silver metal by reduction of Ag^+ to Ag^0 started after ~0.37 electron equivalents were added to the structure. The *in situ* formation of silver metal on discharge in $Ag_{0.48}VOPO_4 \cdot 1.9H_2O$ is delayed compared to $Ag_2VO_2PO_4$ where the formation of silver metal is the predominant process upon initial reduction. Additionally, constriction of the vanadium phosphorous oxygen layers is noted on reduction of Ag^+ to Ag^0 in $Ag_{0.48}VOPO_4 \cdot 1.9H_2O$ while this is not observed in the reduction of $Ag_2VO_2PO_4$. Under constant current, lithium anode cells with $Ag_{0.48}VOPO_4 \cdot 1.9H_2O$ cathodes showed two voltage plateaus at 3.7

and 3.2 V and delivered 144 mAh g^{-1} above 2.0 V. This work contributes to the ability to tune electrochemical properties of cathode materials, including bimetallic phosphates, by control of chemical composition and structure.

Acknowledgements

This project was supported by the University at Buffalo (SUNY), National Institutes of Health under Grant 1R01HL093044-01A1 from the National Heart, Lung, and Blood Institute.

References

[1] A. Yamada, M. Hosoya, S.-C. Chung, Y. Kudo, K. Hinokuma, K.-Y. Liu, Y. Nishi, Journal of Power Sources 119–121 (2003) 232–238.
[2] N. Iltchev, Y.K. Chen, S. Okada, J. Yamaki, Journal of Power Sources 119 (2003) 749–754.
[3] K.J. Takeuchi, A.C. Marschilok, S.M. Davis, R.A. Leising, E.S. Takeuchi, Coordination Chemistry Reviews 219–221 (2001) 283–310.
[4] K.J. Takeuchi, A.C. Marschilok, E.S. Takeuchi, Preparation, Characterization, and Battery Applications of Silver Vanadium Oxide Materials, Chapter 13 in: A.S. Tracey, G.R. Willsky, E.S. Takeuchi (Eds.), Vanadium: Chemistry, Biochemistry, Pharmacology and Practical Applications, Taylor and Francis, New York, 2007.
[5] E.S. Takeuchi, K.J. Takeuchi, A.C. Marschilok, in: J. Garche, C. Dyer, P. Moseley, Z. Oguma, D.R.B. Scrosati (Eds.), Encyclopedia of Electrochemical Power Sources, Elsevier, Amsterdam, 2009, pp. 100–110.
[6] R.A. Leising, W.C. Thiebolt, E.S. Takeuchi, Inorganic Chemistry 33 (1994) 5733–5740.
[7] A.C. Marschilok, K.J. Takeuchi, E.S. Takeuchi, Electrochemical and Solid-State Letters 12 (2008) A5–A9.
[8] E.S. Takeuchi, A.C. Marschilok, K. Tanzil, E.S. Kozarsky, S. Zhu, K.J. Takeuchi, Chemistry of Materials 21 (2009) 4934–4939.
[9] A.C. Marschilok, E.S. Kozarsky, K. Tanzil, S. Zhu, K.J. Takeuchi, E.S. Takeuchi, Journal of Power Sources 195 (2010) 6829–6846.
[10] Y.J. Kim, A.C. Marschilok, K.J. Takeuchi, E.S. Takeuchi, Journal of Power Sources (2010), doi:10.1016/j.jpowsour.2010.10.054.
[11] P. Ayyappan, A. Ramanan, C.C. Torardi, Inorganic Chemistry 37 (1998) 3628–3634.
[12] H.Y. Kang, S.L. Wang, P.P. Tsai, K.H. Lii, Journal of the Chemical Society, Dalton Transactions: Inorganic Chemistry (1972–1999) (1993) 1525–1528.
[13] M.E. Arroyo-de Dompablo, P. Rozier, M. Morcrette, J.M. Tarascon, Chemistry of Materials 19 (2007) 2411–2422.